

SUPERNOVA 2008bk AND ITS RED SUPERGIANT PROGENITOR

SCHUYLER D. VAN DYK¹, TIM J. DAVIDGE², NANCY ELIAS-ROSA^{1,3}, STEFAN TAUBENBERGER⁴, WEIDONG LI⁵,
EMILY M. LEVESQUE^{6,11}, STANLEY HOWERTON⁷, GIULIANO PIGNATA⁸, NIDIA MORRELL⁹,
MARIO HAMUY¹⁰, AND ALEXEI V. FILIPPENKO⁵

¹ Spitzer Science Center/Caltech, Mailcode 220-6, Pasadena, CA 91125, USA; vandyk@ipac.caltech.edu

² Herzberg Institute of Astrophysics, National Research Council of Canada, Victoria, B.C., V9E 2E7, Canada; tim.davidge@nrc.ca

³ Institut de Ciències de l'Espai (IEEC-CSIC), Facultat de Ciències, Campus UAB, 08193 Bellaterra, Spain; nelias@ieec.cat

⁴ Max-Planck-Institut für Astrophysik, Karl-Schwarzschild-Str. 1, 85741 Garching bei München, Germany; tauben@mpa-garching.mpg.de

⁵ Department of Astronomy, University of California, Berkeley, CA 94720-3411, USA; weidong@astro.berkeley.edu, alex@astro.berkeley.edu

⁶ CASA, Department of Astrophysical and Planetary Sciences, University of Colorado 389-UCB, Boulder, CO 80309, USA; Emily.Levesque@colorado.edu

⁷ 1401 South A, Arkansas City, KS 67005, USA; watchingthesky2003@yahoo.com

⁸ Departamento de Ciencias Físicas, Universidad Andres Bello, Avda. Republica 252, Santiago, Santiago RM, Chile; gpignata@unab.cl

⁹ Las Campanas Observatory, Carnegie Observatories, Casilla 601, La Serena, Chile; nmorrell@lco.cl

¹⁰ Departamento de Astronomía, Universidad de Chile, Casilla 36-D, Santiago, Chile; mhamuy@das.uchile.cl

Received 2010 November 24; accepted 2011 November 2; published 2011 December 9

ABSTRACT

We have obtained limited photometric and spectroscopic data for supernova (SN) 2008bk in NGC 7793, primarily at $\gtrsim 150$ days after explosion. We find that it is a Type II-Plateau (II-P) SN that most closely resembles the low-luminosity SN 1999br in NGC 4900. Given the overall similarity between the observed light curves and colors of SNe 2008bk and 1999br, we infer that the total visual extinction to SN 2008bk ($A_V = 0.065$ mag) must be almost entirely due to the Galactic foreground, similar to what has been assumed for SN 1999br. We confirm the identification of the putative red supergiant (RSG) progenitor star of the SN in high-quality $g'r'i'$ images we had obtained in 2007 at the Gemini-South 8 m telescope. Little ambiguity exists in this progenitor identification, qualifying it as the best example to date, next to the identification of the star Sk $-69^\circ 202$ as the progenitor of SN 1987A. From a combination of photometry of the Gemini images with that of archival, pre-SN, Very Large Telescope JHK_s images, we derive an accurate observed spectral energy distribution (SED) for the progenitor. We find from nebular strong-intensity emission-line indices for several H II regions near the SN that the metallicity in the environment is likely subsolar ($Z \approx 0.6 Z_\odot$). The observed SED of the star agrees quite well with synthetic SEDs obtained from model RSG atmospheres with effective temperature $T_{\text{eff}} = 3600 \pm 50$ K. We find, therefore, that the star had a bolometric luminosity with respect to the Sun of $\log(L_{\text{bol}}/L_\odot) = 4.57 \pm 0.06$ and radius $R_\star = 496 \pm 34 R_\odot$ at ~ 6 months prior to explosion. Comparing the progenitor's properties with theoretical massive-star evolutionary models, we conclude that the RSG progenitor had an initial mass in the range of $8\text{--}8.5 M_\odot$. This mass is consistent with, albeit at the low end of, the inferred range of initial masses for SN II-P progenitors. It is also consistent with the estimated upper limit on the initial mass of the progenitor of SN 1999br, and it agrees with the low initial masses found for the RSG progenitors of other low-luminosity SNe II-P.

Key words: galaxies: individual (NGC 7793) – stars: evolution – stars: fundamental parameters – stars: late-type – supernovae: general – supernovae: individual (SN 2008bk)

1. INTRODUCTION

The evolution of massive stars, particularly their endpoints, remains a fascinating, and still unresolved, set of questions and problems that have ramifications in various aspects of astrophysics, such as galactic evolution and chemical enrichment. Theoretically, we expect stars with initial masses greater than $8\text{--}9 M_\odot$ to terminate central nuclear burning while in the red supergiant (RSG) phase of their evolution, undergo core collapse, and explode as supernovae (SNe; Woosley & Weaver 1986; Heger et al. 2003). From observations of the progenitor stars of Type II-Plateau (II-P) SNe, we find that this theoretical lower mass limit is essentially what is being inferred (Smartt et al. 2009). The SNe II-P from detected stars near this limit have tended to be of relatively low luminosity, such as SN 2005cs in M51 (Maund et al. 2005; Li et al. 2006) and SN 2009md in NGC 3389 (Fraser et al. 2011). This stands in contrast to models which argue that low-luminosity SNe II-P can be explained by fallback of ejecta on a newly formed black hole, as a result

of the core collapse of a highly massive ($\gtrsim 20 M_\odot$) progenitor (e.g., Turatto et al. 1998; Zampieri et al. 2003; Nomoto et al. 2006).

In recent years, SN progenitors have been directly identified in pre-SN archival images obtained by the *Hubble Space Telescope* (*HST*). Of course, direct progenitor identification has also been made from the ground prior to that, the most famous example being the discovery of the star Sk $-69^\circ 202$ as the progenitor of SN 1987A in the Large Magellanic Cloud (LMC; e.g., Gilmozzi et al. 1987; Sonneborn et al. 1987). Other cases include the progenitors of SN 1961V in NGC 1058 (Bertola 1964; Zwicky 1964), SN 1978K in NGC 1313 (Ryder et al. 1993), and SN 1993J in M81 (Aldering et al. 1994; Cohen et al. 1995; Van Dyk et al. 2002). However, all of these examples are SNe that in some way have been peculiar or otherwise unusual. The nature of SN 1961V as a true SN continues to be debated (see Van Dyk 2005, and references therein; also, Smith et al. 2011; Kochanek et al. 2011; Van Dyk & Matheson 2011).

SN 2008bk in the nearby, nearly face-on spiral galaxy NGC 7793 (see Figure 1) has also had its progenitor star identified in ground-based data. The SN was discovered by

¹¹ Einstein Fellow

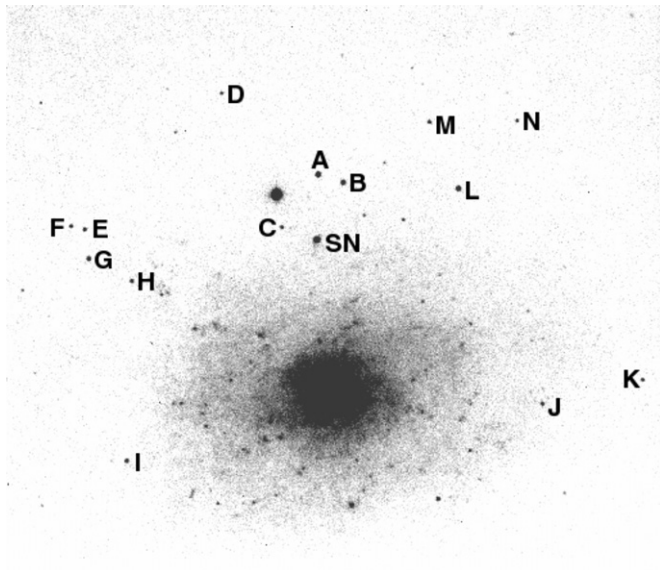


Figure 1. Chart of SN 2008bk in NGC 7793 in an *I*-band image obtained with the Calar Alto 2.2 m telescope on 2008 September 13. The comparison stars from Table 1, as well as the SN, are labeled. North is up and east is to the left.

Monard (2008) on March 25.14 (UT dates are used throughout this paper). Li et al. (2008) were the first to attempt to identify the progenitor star as a likely RSG in deep archival ground-based *BVI* images obtained in 2001 with one of the 8.2 m Unit Telescopes (UT) of the European Southern Observatory (ESO) Very Large Telescope (VLT). They used the Monard discovery images and also images taken on March 28.41 with the 0.41 m PROMPT 2 telescope at the Cerro Tololo Inter-American Observatory (CTIO) as references. This search for the progenitor was attempted even before the SN had been classified. However, Li et al. concluded that SN 2008bk was likely a core-collapse SN, since a star was detected at the location; it is far less likely that we would be able to detect the progenitor, or the companion to the progenitor, of a thermonuclear Type Ia SN outside of the Local Group (see, e.g., Li et al. 2011). The SN was subsequently classified by Morrell & Stritzinger (2008) as Type II with an age of 36 days after explosion on April 12.4, based on a comparison with the well-studied SN II-P 1999em in NGC 1637.

Maoz & Mannucci (2008) detected and measured magnitudes for the progenitor star in archival near-infrared (IR) *J*- and *K_s*-band images, also obtained with the VLT in 2005. Mattila et al. (2008) further analyzed the VLT optical images, as well as VLT *H*-band data obtained in 2007, and combined these pre-SN results with precise astrometry provided by post-SN *K_s* VLT adaptive optics imaging. From their analysis they concluded that the total extinction toward the progenitor is $A_V = 1.0 \pm 0.5$ mag, and that the star therefore was likely of type M4 I, with an initial mass of $8.5 \pm 1.0 M_{\odot}$.

In this paper, with limited photometry and spectroscopy of the SN itself, we show that SN 2008bk is an SN II-P very similar to the low-luminosity SN 1999br in NGC 4900 (Pastorello et al. 2004). Furthermore, we measure accurate photometry for the RSG progenitor from superior-quality *g'r'i'* images obtained in 2007 with the Gemini-South 8 m telescope, as well as from the archival, pre-SN, near-IR VLT images. We compare this photometry to spectral energy distributions (SEDs) obtained from stellar atmosphere models for RSGs to infer the star's effective temperature. Together with the inferred luminosity for the star, we compare these properties to recent theoretical

models for massive-star evolution to estimate the initial mass for the progenitor. We also compare our results to those obtained by Mattila et al. (2008).

2. SUPERNOVA OBSERVATIONS

Although highly incomplete in terms of photometric and spectroscopic coverage, our observations of SN 2008bk are still sufficient to determine its general properties and to allow for comparison with other SNe II. A more complete analysis of the properties of SN 2008bk is forthcoming (G. Pignata et al. 2012, in preparation).

2.1. Photometry

We obtained *BVRI* images of SN 2008bk, at eight epochs late in its evolution: four at the Calar Alto 2.2 m telescope + the CAFOS SiTe (scale $0''.53 \text{ pixel}^{-1}$, field of view $9' \times 9'$), two at the 2.5 m Nordic Optical Telescope (NOT; Roque de los Muchachos Observatory, La Palma, Spain) + ALFOSC ($0''.19 \text{ pixel}^{-1}$, field of view $6'.5 \times 6'.5$), and two using the SMARTS 1.3 m telescope + ANDICAM at CTIO. These images were processed using standard IRAF¹² procedures for image trimming, bias subtraction, and flat-field corrections. Additionally, we add several relatively early-time epochs at *V*, with an image obtained at the Las Campanas Observatory (LCO) 2.5 m duPont telescope on 2008 April 13 and six images obtained with the Global Rent-A-Scope (GRAS) 0.32 m and 0.41 m telescopes at epochs spanning the plateau to early on the exponential tail. We have also included *BV* data, obtained by the Chilean Automatic Supernova sEarch (CHASE; Pignata et al. 2008) with PROMPT 2.

We extracted instrumental photometry for the SN and reference stars from these images, generally, via point-spread function (PSF) fitting using DAOPHOT (Stetson 1987) within IRAF. When the shapes of the stars in images deviated substantially from a “well-behaved” PSF, we relied only on aperture photometry. For this reason, we calibrated the SN and reference star instrumental photometry from all of the images to existing photometry for the star field around the host galaxy. NGC 7793 was observed by Larsen & Richtler (1999) in *UBVRI* with the Danish 1.54 m telescope + the Danish Faint Object Spectrograph and Camera on 1997 September 6. We obtained these images, posted for public distribution in FITS format, from the NASA/IPAC Extragalactic Database (NED¹³). We extracted instrumental magnitudes from the images using IRAF, first with a $4''$ aperture and then with a PSF for each band. Calibration was established using photometry of a number of isolated reference stars through a $20''$ aperture, which matches the aperture used to establish the calibration through standard-star observations by Larsen (1999, his Table 1); see Figure 1 and Table 1 for the locations and magnitudes of these stars. We also applied the appropriate extinction corrections (S. S. Larsen 2010, private communication).

We can compare our *BVR* photometry with those magnitudes provided in NOMAD,¹⁴ however, the uncertainties in these latter magnitudes are substantial, resulting in large scatter in the comparison: for *B*, $\text{NOMAD} - \text{Ours} = -0.32 \pm 0.20$;

¹² IRAF (Image Reduction and Analysis Facility) is distributed by the National Optical Astronomy Observatory, which is operated by the Association of Universities for Research in Astronomy, Inc., under cooperative agreement with the National Science Foundation (NSF).

¹³ <http://nedwww.ipac.caltech.edu>.

¹⁴ <http://www.nofs.navy.mil/nomad.html>.

Table 1
Photometric Sequence around SN 2008bk^a

Star	<i>B</i> (mag)	<i>V</i> (mag)	<i>R</i> (mag)	<i>I</i> (mag)
A	17.459(004)	16.328(003)	15.728(004)	15.085(008)
B	16.939(003)	16.283(003)	15.910(003)	15.447(008)
C	18.894(012)	18.120(015)	17.662(015)	17.132(013)
D	18.574(005)	17.898(003)	17.512(004)	17.045(008)
E	18.184(005)	17.314(003)	16.813(003)	16.290(010)
F	19.415(007)	18.251(003)	17.531(003)	16.832(008)
G	19.025(006)	17.714(003)	16.836(003)	15.861(008)
H	20.092(011)	18.642(004)	17.664(000)	16.561(008)
I	19.392(008)	18.054(003)	17.178(003)	16.219(006)
J	17.512(012)	17.401(012)	17.289(012)	16.918(011)
K	15.013(001)	14.278(018)	15.080(051)	13.497(014)
L	16.794(004)	16.130(004)	15.790(004)	15.364(007)
M	17.515(004)	17.060(004)	16.814(004)	16.444(007)
N	18.730(004)	18.031(004)	17.649(004)	17.165(004)

Note. ^a Uncertainties (1σ) are given in parentheses in units of 0.001 mag.

for *V*, -0.51 ± 0.15 ; and for *R*, -0.39 ± 0.19 . A far better comparison can be made at *I* with the more reliable photometry from the DENIS database (The DENIS Consortium 2005): DENIS – Ours = 0.02 ± 0.05 mag. The good agreement in the *I* magnitudes provides us with some confidence, overall, in the calibration of our photometry.

As many reference stars as possible were generally adopted for the calibration; however, for the shallowest images, we had to use a combination of the magnitudes of star K (the brightest star in Table 1) and the less precise *BV* photometry from the bright NOMAD stars seen in these images. The resulting photometry of SN 2008bk is given in Table 2. The uncertainties in the SN photometry in all four bands arise from the measurement uncertainties from DAOPHOT, the uncertainties in the absolute calibration given by Larsen (1999), and the uncertainties in

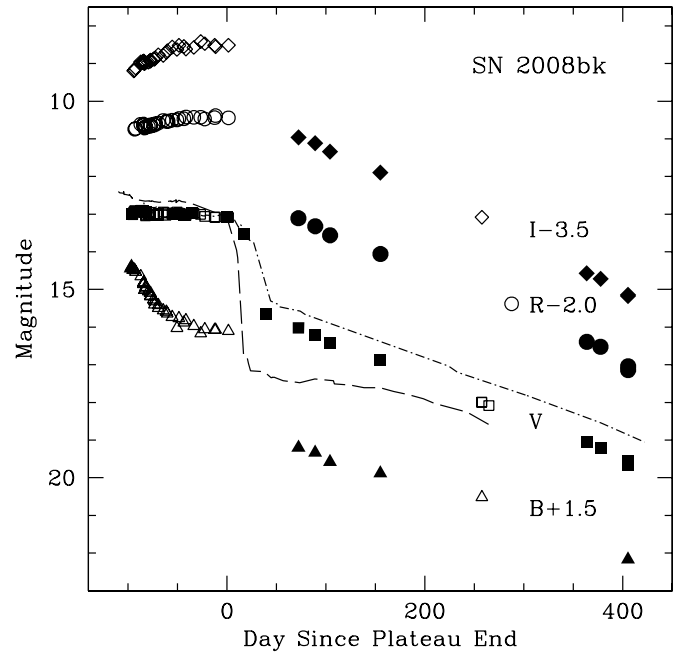


Figure 2. Limited *BVRI* light curves of SN 2008bk from photometry in Table 2 (solid points). Shown for comparison are the light curves for the submilluminous SN II-P 1999br in NGC 4900 (open points; Pastorello et al. 2004), as well as the *V* light curves for the SNe II-P 1999em in NGC 1637 (dot-dashed line; Hamuy et al. 2001; Leonard et al. 2002; Elmhamdi et al. 2003) and 2005cs in M51 (dashed line; Pastorello et al. 2009). These latter comparison light curves have all been adjusted, by eye, in brightness to match the end of the plateau phase for SN 2008bk. All light curves are shown relative to the epoch corresponding to the end of the plateau phase.

transforming the instrumental magnitudes to standard magnitudes, based on the reference stars, all added in quadrature.

The *BVRI* light curves for SN 2008bk are shown in Figure 2. As we have noted, many of the multi-band points are beyond the plateau phase and on the exponential tail. However, the

Table 2
Optical Photometry of SN 2008bk^a

UT Date	JD – 2,450,000	<i>B</i> (mag)	<i>V</i> (mag)	<i>R</i> (mag)	<i>I</i> (mag)	Source ^b
2008 Mar 28.41	4553.90	12.94(13)	CHASE
2008 Mar 29.40	4554.90	12.89(14)	12.99(10)	CHASE
2008 Apr 13.41	4569.91	...	12.94(05)	LCO duPont
2008 May 10.79	4596.29	...	12.99(13)	S. Howerton
2008 May 22.80	4608.30	...	13.02(06)	S. Howerton
2008 May 30.85	4616.35	...	12.97(26)	S. Howerton
2008 Jul 4.80	4651.30	...	13.07(12)	S. Howerton
2008 Jul 21.65	4668.15	...	13.52(13)	S. Howerton
2008 Aug 13.63	4691.13	...	15.64(11)	S. Howerton
2008 Sep 13.02	4723.52	17.70(07)	16.02(06)	15.11(05)	14.46(08)	Calar Alto
2008 Sep 30.93	4740.43	17.83(07)	16.22(06)	15.32(05)	14.62(08)	Calar Alto
2008 Oct 15.91	4755.41	18.08(08)	16.43(06)	15.56(05)	14.84(08)	Calar Alto
2008 Dec 5.84	4806.34	18.38(07)	16.87(06)	16.06(05)	15.40(08)	NOT
2009 Jul 2.37	5014.87	...	19.04(03)	18.39(03)	18.07(03)	SMARTS
2009 Jul 16.36	5028.86	...	19.21(05)	18.52(07)	18.22(03)	SMARTS
2009 Aug 13.13	5056.63	20.67(06)	19.55(08)	19.14(05)	18.67(08)	Calar Alto
2009 Aug 13.16	5056.66	...	19.65(05)	19.04(03)	18.64(03)	NOT

Notes.

^a Uncertainties (1σ) are given in parentheses, in units of 0.01 mag.

^b CHASE: 0.41 m PROMPT2 + Apogee U47; LCO duPont: Las Campanas Observatory 2.5 m duPont + SITE2K; S. Howerton: GRAS-008 + SBIG ST-L-11K 3, GRAS-015 + SBIG ST-8 3, or SBIG ST-10 3 CCD; Calar Alto: 2.2 m Calar Alto + CAFOS; NOT: 2.5 m Nordic Optical Telescope + ALFOSC; SMARTS: 1.3 m SMARTS + ANDICAM.

Table 3
Optical Spectroscopy of SN 2008bk

UT Date	JD – 2,450,000	Day ^a	Grism/Grating	Wavelength Range (Å)	Instrument ^b
2008 Jul 23.36	4670.86	20	KPGL3-1	4005–7738	CTIO
2008 Jul 24.35	4671.85	21	KPGL3-1	4005–7738	CTIO
2008 Jul 25.31	4672.81	22	KPGL3-1	4005–7738	CTIO
2008 Sep 14.04	4723.54	72	G200	4900–10458	CAHA
2008 Sep 16.02	4725.52	74	G200	3665–10463	CAHA
2008 Sep 30.93	4740.43	89	R100	5710–9585	CAHA

Notes.

^a The approximate day is referenced to our estimate of the end of the plateau phase, JD \approx 2,454,651.3.

^b CTIO: Blanco 4 m telescope + R-C Spec (Cerro Tololo, Chile); CAHA: Calar Alto 2.2 m telescope + CAFOS SiTe (near Almeria, Spain).

V photometry at earlier times provides us with adequate leverage on the overall photometric evolution of SN 2008bk, from soon after explosion through the onset of this tail. The lone early-time $B - V$ data point provides us with some leverage on the initial color of the SN.

For comparison, we also show in Figure 2 the V light curves for both the “normal” SN II-P 1999em (Hamuy et al. 2001; Leonard et al. 2002; Elmhamdi et al. 2003) and the subluminal SN II-P 2005cs in M51 (Pastorello et al. 2009), and, for all bands, the subluminal SN II-P 1999br (Pastorello et al. 2004). We have attempted to match, by eye, the brightnesses of these comparison SNe with SN 2008bk toward the end of the plateau phase at V . Although we have very limited coverage at the end of the plateau, it appears that this phase ended very near JD 2,454,651 (i.e., 2008 July 3), implying that the plateau lasted \sim 100 days after discovery. (Additionally, the end of the plateau phase for SN 1999br is not well defined; Pastorello et al. 2004.) The SN 2008bk light curves are shown in Figure 2 relative to that epoch.

In Figure 3, we show the absolute V light curve for SN 2008bk, which results from correcting for the assumed extinction (see Section 4.1) and distance modulus (see Section 4.2) to the SN. We also show for comparison the absolute V light curves for SN 1999em, corrected for the total extinction, $A_V = 0.31$ mag (e.g., Hamuy et al. 2001), and the Cepheid distance modulus to its host galaxy (Leonard et al. 2003); SN 2005cs, corrected for the extinction from Pastorello et al. (2009) and the distance modulus from Tonry et al. (2001); and SN 1999br (extinction and distance modulus from Pastorello et al. 2004). We estimate that SN 2008bk had an absolute magnitude near maximum brightness during the plateau phase of $M_V^0 = -14.8$ mag, which is \sim 2.1 mag less luminous than SN 1999em. Although the plateau brightness for SN 2008bk is very similar to the $M_V^0 = -14.9$ mag for the low-luminosity SN II-P 2005cs (Pastorello et al. 2009), SN 2008bk did not decline nearly as rapidly, post-maximum, nor is it nearly as subluminal on the tail as SN 2005cs. One can see from Figure 2 that SN 2008bk exhibits a striking photometric resemblance to SN 1999br at all bands. However, a noticeable offset exists between the absolute brightnesses of SNe 2008bk and 1999br; we comment on this more in Section 5. We will demonstrate in Section 2.2 that SN 2008bk also spectroscopically most closely resembles SN 1999br. We therefore consider SN 2008bk to be a low-luminosity SN II-P, quite similar to SN 1999br.

The photometric comparison with SN 1999br (assuming the explosion date for SN 1999br is JD 2,451,278; Pastorello et al. 2004) indicates that the explosion epoch for SN 2008bk was

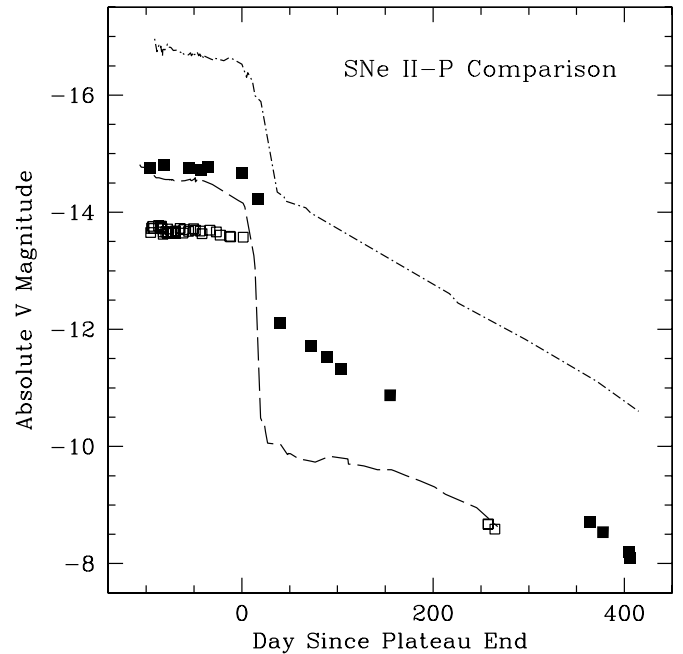


Figure 3. Evolution of the absolute V magnitude of SN 2008bk (solid points). Shown for comparison are the absolute V light curves for the subluminal SN II-P 1999br in NGC 4900 (open points; Pastorello et al. 2004), as well as for the SNe II-P 1999em in NGC 1637 (dot-dashed line; Hamuy et al. 2001; Leonard et al. 2002; Elmhamdi et al. 2003) and 2005cs in M51 (dashed line; Pastorello et al. 2009). The observed V light curves for the SNe have been corrected for their respective extinction and distance; see the text. All light curves are shown relative to the epoch corresponding to the end of the plateau phase.

\sim JD 2,454,550, or \sim 2008 March 24. Monard, therefore, likely discovered the SN \lesssim 1 day after explosion.

2.2. Spectroscopy

We obtained several spectra of SN 2008bk at late times, using the Blanco 4 m telescope at CTIO with the RC-Spectrograph in 2008 July and using the Calar Alto 2.2 m telescope with the CAFOS SiTe imaging spectrograph in 2008 September. The details of these observations are given in Table 3. The spectra were reduced using standard IRAF routines. The preprocessing of the spectroscopic data (trimming, bias, overscan, and flat-field correction) were the same as for the images (see Section 2.1). The one-dimensional spectra were wavelength calibrated by comparison with arc-lamp spectra obtained during the same night and with the same instrumental configuration, and flux calibrated using spectrophotometric standard stars. The zero

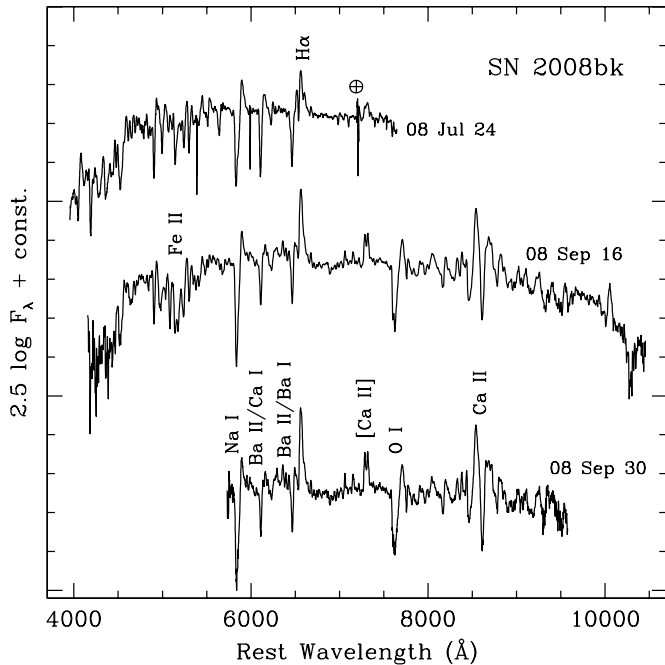


Figure 4. Optical spectra of SN 2008bk obtained with the 4 m CTIO Blanco telescope on 2008 July 24, and with the 2.2 m Calar Alto telescope on 2008 September 16 and 30. See Table 3 and the text. Several notable features in the spectra are indicated.

point of the wavelength calibration was verified against the bright night-sky emission lines. The standard-star spectra were also used to model and remove the telluric absorption (e.g., Matheson et al. 2000).

The resulting spectra are shown in Figure 4. Since the spectra obtained at CTIO are only spaced in time each by a day, the features in the spectra had varied little in that time interval. Thus, we show only a representative spectrum from July 24. The same is true for the two spectra obtained at Calar Alto in mid-September; we display only the spectrum from September 16. The July 24 spectrum is ~ 21 days past the plateau phase, while the September 16 and 30 spectra are during the nebular phase, at ~ 75 and ~ 89 days past the plateau. In Figure 5, we show the SN 2008bk spectrum from July 24, and also spectra of the normal SN II-P 1999em (Leonard et al. 2002) at 1 day and 29 days past the plateau phase, as well as a spectrum of the subluminous SN II-P 1999br in NGC 4900 (Pastorello et al. 2004) at essentially the end of the plateau. The spectra for SN 1999em were obtained from the SUSPECT SN database.¹⁵ A. Pastorello kindly provided the spectrum from the Padova SN data archive of SN 1999br from 1999 July 20.

Both the strength and width of the various spectral lines, and the overall continuum shape, for SN 2008bk compare rather poorly with SN 1999em. A far better comparison, overall, can be made with SN 1999br. The relative strength of, for example, the [Ca II] $\lambda\lambda 7291, 7324$ feature in the SN 2008bk spectrum, compared with that in the SN 1999br spectrum, again indicates that SN 2008bk is also a low-luminosity SN II-P.

3. DETECTION OF THE PROGENITOR STAR

Li et al. (2008) measured a precise position for the SN of $\alpha(\text{J2000}) = 23^{\text{h}}57^{\text{m}}50^{\text{s}}.42$, $\delta(\text{J2000}) = -32^{\circ}33'21''.5$. Within the uncertainty of this position ($\pm 0''.2$) they isolated a star in the VLT

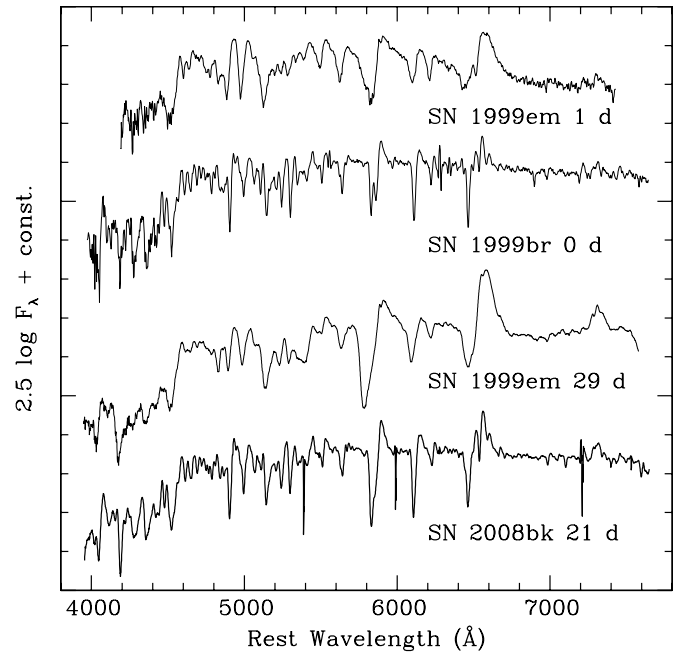


Figure 5. Comparison of the SN 2008bk optical spectrum from 2008 July 24 (see Table 3) with the spectra of SN 1999em (Leonard et al. 2002) and a spectrum of SN 1999br (Pastorello et al. 2004). The ages, in days, for the SNe in the figure are relative to the estimated epoch for the end of the photometric plateau phase in each case.

I-band image at this location. The star is not detected in the *B* and *V* images from the same epoch. This candidate progenitor lies within a prominent cluster of bright blue and red supergiant stars. From its environment and its lack of detection in the bluer bands, Li et al. conjectured that the progenitor was an RSG.

We have since improved the astrometric agreement, with an uncertainty of $0''.13$, between the SN and the star with a *V* image of the SN from the LCO 2.5 m duPont telescope, obtained on 2008 April 13. We have refined the absolute position for the SN to end figures 50.50 s and $20''.7$ (with uncertainty $\pm 0''.2$).

We obtained deep *g'r'i'* images in 2007 September and October with GMOS (Crampton et al. 2000) on Gemini-South to study the outer disk of NGC 7793. The images were obtained in queue observing mode as part of program GS2007B-Q-57 (PI: Davidge). The detector in GMOS is a mosaic of three CCDs with a raw image scale of $0''.0727 \text{ pixel}^{-1}$. The data were binned $2 \times 2 \text{ pixels}^2$ to better match the delivered image quality. Eight 200 s exposures were obtained in *g'* and eight 300 s exposures were obtained in both *r'* and *i'*. The raw images in each band were bias subtracted, divided by a twilight flat, and then stacked. The progenitor star and its environment are shown in Figure 6. From these images we measure an absolute position for the star to end figures 50.48 s and $20''.9$ ($\pm 0''.2$). To within the absolute astrometric uncertainties, the position of the identified progenitor star agrees very well with the SN position (see above).

We extracted instrumental photometry from the *g'r'i'* images via PSF fitting within IRAF/DAOPHOT. Since the Gemini program was intended to be carried out during nonphotometric conditions as part of the so-called Poor Weather Queue, this photometry must be calibrated using other observations. Following Welch et al. (2007), we then transformed the *g'r'i'* instrumental magnitudes from the Gemini images to the calibrated *VRI* magnitudes from the Danish telescope images (see Section 2.1), using a number of bright ($V = 16.1\text{--}20.4 \text{ mag}$),

¹⁵ <http://suspect.nhn.ou.edu/~suspect>.

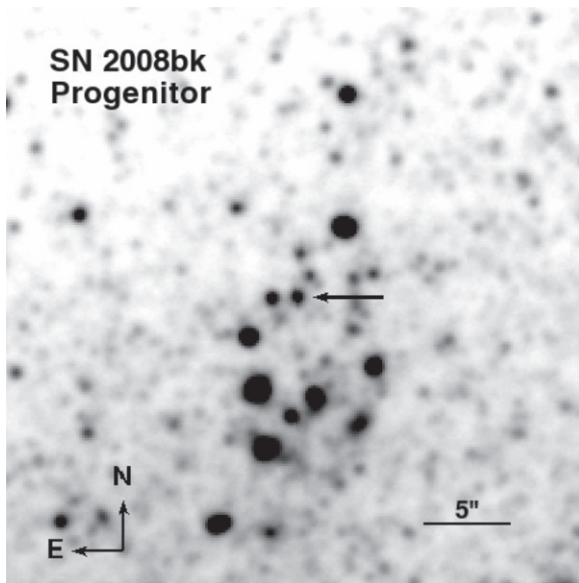


Figure 6. Co-added i' -band image, from data obtained in 2007 September and October with the Gemini-South GMOS imager, showing the confirmed RSG progenitor of SN 2008bk (indicated by the arrow). The area of the image displayed here is $33'' \times 33''$. The effective seeing in the combined image is $\sim 0''.65$.

isolated stars common to both sets of images. The resulting transformations are

$$V = 0.7803g' - 0.0181r' + 0.2768i' + \text{zero point},$$

$$R = 0.0000g' + 0.7762r' + 0.2419i' + \text{zero point},$$

$$I = 0.0000g' - 0.0722r' + 1.1055i' + \text{zero point}.$$

We note that the coefficients in the transformation above are similar to the ones derived by Welch et al. as applied to a different scientific context. The uncertainties in these transformations are 0.08 mag for V , 0.05 mag for R , and 0.07 mag for I .

The resulting VRI magnitudes for the SN 2008bk progenitor from the Gemini images are given in Table 4. The uncertainties in the magnitudes include the measurement uncertainties from DAOPHOT, the uncertainties in the calibration of the Danish telescope images of the galaxy (Larsen 1999, his Table 1), and the uncertainties in the transformations above, all added in quadrature.

We also reanalyzed and remeasured the photometry from the near-IR VLT ISAAC and HAWK-I JHK_s images, initially analyzed by Maoz & Mannucci (2008) and Mattila et al. (2008). Photometry was performed, again using PSF fitting with IRAF/DAOPHOT, and the instrumental magnitudes were calibrated to Two Micron All Sky Survey (2MASS) stars in the fields. The resulting photometry is given in Table 4. The uncertainties in the magnitudes include the measurement uncertainties from DAOPHOT, the uncertainties in the 2MASS star magnitudes, and the uncertainties in the transformations using 2MASS. Later (see Section 4.4), we will need these near-IR magnitudes in the Bessell & Brett (1988) system, particularly for K . For this reason, we use the transformations from the 2MASS system in Carpenter (2001, his Appendix A) to obtain $J = 19.34$, $H = 18.56$, and $K = 18.18$ mag (formal uncertainties in these transformations are all < 0.01 mag).

Table 4
Photometry of the SN 2008bk Progenitor

Band	Magnitude
V	22.81(09)
R	22.03(07)
I	20.71(08)
J	19.26(14)
H	18.55(06)
K_s	18.14(10)

Notes. Uncertainties (1σ) are given in parentheses, in units of 0.01 mag. The JHK_s magnitudes are in the 2MASS photometric system.

4. PROPERTIES OF THE PROGENITOR STAR AND ITS ENVIRONMENT

We will now place the SN 2008bk progenitor in a Hertzsprung–Russell diagram (HRD) to attempt to estimate its initial mass. Whereas the photometry of the progenitor star has relatively small uncertainties, the next steps, discussed below, involved in analyzing this photometry possess significantly larger uncertainties.

4.1. Extinction to the Supernova

Here we estimate the extinction to the SN. The startlingly good agreement, seen in Figure 2, between the light curves of both SN 2008bk and SN 1999br in all observed bands (the SN 1999br curves have all been uniformly adjusted by -4.6 mag to match, by eye, those of SN 2008bk) implies that the extinction toward SN 2008bk is quite similar to that of SN 1999br. Smartt et al. (2009) assume only the Galactic foreground contribution to the extinction toward SN 1999br: $A_V = 0.065$ mag. We can then logically infer that the extinction toward SN 2008bk is comparably quite low; we assume $A_V = 0.065$ mag. Interestingly, the estimate for the Galactic line-of-sight extinction toward the SN is, in fact, $A_V = 0.065$ mag (Schlegel et al. 1998), which would imply that the extinction in the immediate galactic environment of SN 2008bk is negligible. From a preliminary analysis of the photospheric spectra for SN 2008bk, no sign exists of Na I D absorption due to the host galaxy. Additionally, the average internal extinction in NGC 7793 is generally quite low ($A_B = 0.12$ mag; Pierce & Tully 1992). The low-extinction value is consistent with the lack of emission at $8.0 \mu\text{m}$ (normally attributed to emission from polycyclic aromatic hydrocarbons in interstellar dust clouds) detected at the position of SN 2008bk in archival images of NGC 7793 obtained using the InfraRed Array Camera (IRAC) on the *Spitzer Space Telescope*. It is also consistent with the fact that the SN is within what appears to be a nebular, possibly evacuated, bubble (see Figure 7).

4.2. Distance Modulus to the Host Galaxy

We also require an estimate of the distance modulus to the SN. Puche & Carignan (1988) calculated a mean distance modulus, 27.64 ± 0.19 mag, to NGC 7793 from several distance indicators, including the Tully–Fisher relation. Karachentsev et al. (2003) measured a distance modulus of 27.96 ± 0.24 Mpc (somewhat more distant, but in good agreement with the Puche & Carignan value), using *HST* images of the host galaxy to estimate the “tip of the red giant branch” (TRGB) brightness to be $I = 23.95 \pm 0.22$ mag. (These *HST* images, unfortunately, did not cover the SN site; furthermore, we note that Mould &

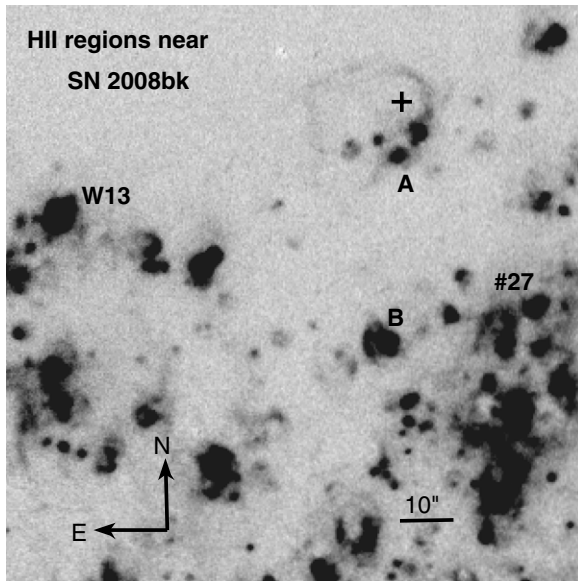


Figure 7. Continuum-subtracted $H\alpha$ ($+[\text{N II}]$) image of NGC 7793, an archival ancillary data product released by the *Spitzer* SINGS project (Kennicutt et al. 2003), with the position of SN 2008bk indicated by a cross. The locations of H II regions near the SN are labeled. Regions “A” and “B” were also detected in a spectrum of SN 2008bk we obtained with the 2.2 m Calar Alto telescope on 2008 September 30. Region “#27” is from Bibby & Crowther (2010). Region W13 is from McCall et al. (1985). See Table 5. Note that the SN site appears to be within a faint, but extended, bubble of ionized gas, of diameter ~ 530 pc. North is up and east is to the left.

Sakai (2008), using the TRGB calibration of $M_I^0 = -4.05$ mag by Rizzi et al. (2007), found $\mu^0 = 27.78$ mag; however, their assumed I -band extinction, $A_I = 0.22$ mag, is almost certainly too large.)

The distance modulus has been recently determined using Cepheids in the host galaxy by Pietrzyński et al. (2010) to be $\mu^0 = 27.68 \pm 0.05$ mag (random) ± 0.08 mag (systematic). Those authors note that their distance modulus also agrees very well with a recent TRGB measurement, $\mu^0 = 27.72 \pm 0.08$ mag, by Jacobs et al. (2009). Hereafter, we adopt the Cepheid distance modulus and, conservatively, assume the (larger) systematic uncertainty in that estimate.

4.3. Metallicity of the Supernova Environment

Furthermore, we need to know the metallicity in the SN environment, since we are comparing the progenitor’s observed characteristics with estimates from models that are generated assuming a particular metallicity.

We consider the metallicity to be equivalent to the local oxygen abundance. The most accurate estimate of the metallicity ideally would be from the immediate SN environment itself, or failing that, from regions of the host galaxy in the general vicinity of the SN. We show several such H II regions in Figure 7, which is a continuum-subtracted $H\alpha$ ($+[\text{N II}]$) image of NGC 7793, released as an ancillary data product by the *Spitzer* SINGS Legacy project¹⁶ (Kennicutt et al. 2003). In the spectroscopic observations of the SN obtained on 2008 September 30 at Calar Alto, light from two H II regions, “A” and “B,” approximately to the south of the SN also fell within the CAFOS slit.

Pettini & Pagel (2004) calibrate relations between the O abundance and the strong-intensity line indices $\text{N2} = \log([\text{N II}] \lambda 6584/H\alpha)$ (see, e.g., Terlevich et al. 1991; Storchi-Bergmann

et al. 1994; Denicoló et al. 2002) and $\text{O3N2} = \log([\text{O III}] \lambda 5007/H\beta)/([\text{N II}] \lambda 6584/H\alpha)$. These two indices are relatively unaffected by extinction, since they depend on ratios of intensities for two spectral lines essentially contiguous in wavelength. The 1σ uncertainties in the O abundance from these two indices are ± 0.18 and ± 0.14 dex, respectively (Pettini & Pagel 2004). We measured the intensities for these various emission lines, using standard routines in IRAF, and estimate these line indices for these two H II regions.

The resulting values of the indices and the computed abundances are given in Table 5. We estimate that our measurement errors lead to uncertainties in the abundances of, conservatively, ± 0.05 dex. Additionally, we can consider the measurements for the H II regions #27 from Bibby & Crowther (2010) and W13 from McCall et al. (1985). These two regions are labeled in Figure 7 and listed in Table 5. We also include in the table the deprojected angular distance of each H II region from the SN, assuming the values of the host-galaxy inclination and position angle from Bibby & Crowther (2010) and references therein. The linear distances in the table are assuming a distance to the host galaxy of 3.4 Mpc (see Section 4.2).

One can see that the O abundances of these H II regions are all consistent with an approximate range of 8.4–8.5 dex. The region nearest to (~ 200 pc from) the SN, in particular, has $12 + \log(\text{O}/\text{H}) = 8.45$. Assuming the solar photospheric abundance is $12 + \log(\text{O}/\text{H}) = 8.66 \pm 0.05$ (Asplund et al. 2004), we can infer that the metallicity in the SN environment is ≈ 0.6 solar. The mean O abundance of H II regions in the LMC is $12 + \log(\text{O}/\text{H}) = 8.37 \pm 0.22$ (Russell & Dopita 1990) or ~ 0.5 solar. Therefore, the metallicity at the SN site is most likely not solar, but also is likely not quite as low as the mean LMC nebular metallicity. However, with the level of uncertainties in the Pettini & Pagel (2004) calibration relations, in our measurements, and in the assumed solar and LMC O abundances, we analyze the progenitor photometry considering a range of metallicities. We will show that the inferred intrinsic properties for the progenitor, nonetheless, are most consistent with subsolar metallicity in the SN environment.

4.4. Initial Mass of the Progenitor

We have assumed a relatively low extinction toward SN 2008bk, based on the comparison with SN 1999br (Section 2.1). We further assume that this extinction (Section 4.1) is also appropriate to apply to the progenitor star. From the Gemini optical data, this star, therefore, had an absolute magnitude $M_V^0 = -4.94$ and a dereddened color $(V - I)_0 \approx 2.19$ mag, which imply that the progenitor was a lower-luminosity (class Ib), early M-type RSG (e.g., Humphreys & McElroy 1984).

From the observed optical and near-IR photometry in Table 4, we show the SED of the star in Figure 8. For comparison we show synthetic SEDs, generated using SYNPHOT applied to the MARCS¹⁷ model stellar atmospheres (Gustafsson et al. 2008) for RSGs with effective temperature $T_{\text{eff}} = 3600$ K and surface gravity $\log g = 0.0$, assuming spherical geometry and subsolar metallicity ($[\text{M}/\text{H}] = -0.25$, where $[\text{M}/\text{H}]$ denotes the ratio of the general metal abundance to H, relative to the Sun). We also show the models at solar metallicity ($[\text{M}/\text{H}] = 0$) for this temperature, and one can see little difference with the subsolar models. The MARCS models are for stars with initial masses 5 and 15 M_{\odot} (we will show that the

¹⁶ Available at <http://irsa.ipac.caltech.edu>.

¹⁷ <http://marcs.astro.uu.se/>

Table 5
Strong-line Indices and Oxygen Abundances^a for H II Regions Near SN 2008bk

Region	SN Offset (") ^b	SN Offset (pc) ^c	N2	12 + log(O/H)	O3N2	12 + log(O/H)	Source
A	12.3	203	-0.71	8.45	This work
B	95.6	1576	-0.62	8.52	This work
#27	82.2	1355	-0.66	8.53	0.81	8.47	Bibby & Crowther (2010)
W13	103.2	1701	<-0.77	<8.41	>1.10	<8.38	McCall et al. (1985)

Notes.

^a Computed following Pettini & Pagel (2004).

^b Angular distance of the H II region from SN 2008bk, deprojected for the host galaxy's position angle and inclination (adopting the values for these from Bibby & Crowther 2010). See Figure 7.

^c Assuming a distance to the host galaxy of 3.4 Mpc (Pietrzyński et al. 2010).

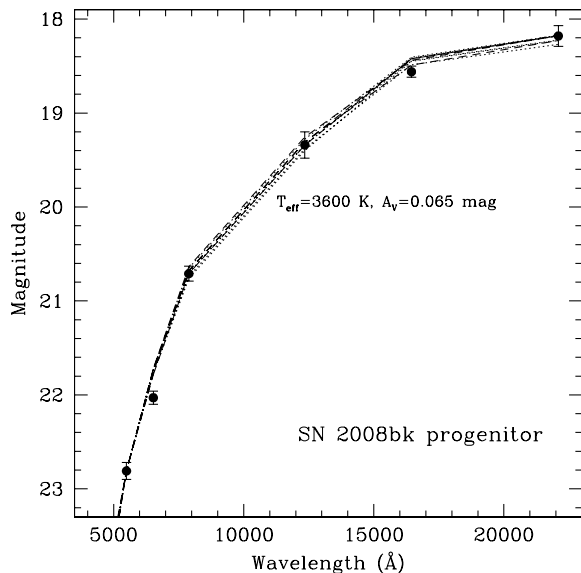


Figure 8. Observed spectral energy distribution (SED) of the SN 2008bk progenitor star (filled circles). For comparison, we also show SEDs based on IRAF/SYNPHOT synthetic photometry extracted from the MARCS model stellar atmospheres (Gustafsson et al. 2008) at $T_{\text{eff}} = 3600$ K of 5 and 15 M_{\odot} stars ($\log g = 0.0$) at solar metallicity ($[M/H] = 0$) with microturbulence velocities of 1–5 km s^{-1} (dashed lines), and at subsolar metallicity ($[M/H] = -0.25$) with microturbulence velocities of 2 and 5 km s^{-1} (dotted lines). We have reddened the model SEDs by our assumed value toward the SN (Section 4.1). The models were also normalized to the observed brightness of the progenitor in V .

initial mass of the SN 2008bk progenitor was between these two values) and have microturbulence velocities spanning from 1 to 5 km s^{-1} . The models were all reddened by the assumed value for the progenitor, following the Cardelli et al. (1989) reddening law, and were normalized to the observed V magnitude. The agreement of all of these models with the observed SED is quite good, to within the uncertainties in the photometry of the progenitor. (However, the models do diverge by $\gtrsim 1\sigma$ from the observation at R , and compare less well with the observations at H .) We therefore consider the effective temperature of the star to be $T_{\text{eff}} = 3600$ K, with a conservative uncertainty of ± 50 K.

This effective temperature corresponds to spectral type M2–M2.5 at LMC metallicity (Levesque et al. 2006, their Table 4) and M3 at solar metallicity (Levesque et al. 2005, their Table 5). The metallicity in the SN 2008bk environment is likely somewhere in between (Section 4.3). From Levesque et al. (2005, their Table 6) for Galactic (solar metallicity) RSGs, the V and K bolometric corrections at $T_{\text{eff}} = 3600$ K are $BC_V = -1.75$ and $BC_K = 2.84$ mag, respectively. At LMC

metallicity, the bolometric corrections vary little from the solar values at this T_{eff} : $BC_V = -1.78$ and $BC_K = 2.84$ mag (Levesque et al. 2006). The absolute bolometric magnitude of the star, therefore, from V is $M_{\text{bol}} = -6.70 \pm 0.12$ mag, and from K it is $M_{\text{bol}} = -6.67 \pm 0.13$ mag. The total uncertainties arise from the uncertainties in the measured photometry for the star and in the distance modulus (see Section 4.2), and at V , in the range in BC_V . That these two estimates of M_{bol} , established from the two different photometric measurements, agree so well to within the uncertainties, instills us with considerable confidence in the star's photometry and in our estimates of the extinction and the star's effective temperature. Assuming $M_{\text{bol}(\odot)} = 4.74$ mag, the bolometric luminosity relative to the Sun is then $\log(L_{\text{bol}}/L_{\odot}) = 4.57 \pm 0.06$ from both V and K . The luminosity and effective temperature together indicate that the RSG's radius, at ~ 6 months prior to explosion, is $R_{\star} = 496 \pm 34 R_{\odot}$.

The inferred intrinsic properties of the progenitor of SN 2008bk are shown in the HRD in Figure 9. We can also compare the star's locus in the HRD with massive-star evolutionary tracks of various initial masses, and, given the uncertainties mentioned in Section 4.3, we take into consideration tracks at several metallicities. In panel (a) of the figure, we compare to tracks at solar metallicity ($Z = 0.02$), i.e., the Cambridge STARS tracks from Eldridge & Tout (2004) and the Geneva tracks from Hirschi et al. (2004), which include either stellar equatorial rotation, at $v_{\text{ini}} = 300 \text{ km s}^{-1}$, or no rotation. One can see that these tracks would imply that the initial mass of the progenitor is in the range of ~ 10 – $12 M_{\odot}$. However, these tracks all terminate at cooler effective temperatures and higher luminosities (and larger stellar radii) than is the case for the progenitor. In total, the solar metallicity tracks compare rather poorly with the progenitor's inferred properties, and we consider it unlikely that the larger initial masses implied by these tracks apply to the SN 2008bk progenitor.

In Figure 9, panel (b), we show a comparison with the STARS tracks at $Z = 0.01$ (i.e., at $Z/Z_{\odot} = 0.5$; the Geneva tracks have not been published at subsolar metallicity in this mass range). The 8 and 8.5 M_{\odot} model tracks both terminate with $T_{\text{eff}} = 3567$ K, and with $\log(L_{\text{bol}}/L_{\odot}) = 4.59$ and 4.63 (respectively) and $R_{\star} = 514$ and 541 R_{\odot} (respectively), which are essentially consistent, to within the uncertainties, with those properties of the progenitor. Note that the 9 M_{\odot} model terminates at a luminosity that is higher than the range we have inferred for the progenitor's luminosity. Note also that the 7.5 M_{\odot} track terminates at a much cooler temperature and much higher luminosity, and therefore we can discount it entirely. In panel (c), we compare with the STARS models for $Z = 0.008$ (i.e., $Z/Z_{\odot} = 0.4$), although it is less likely that the metallicity

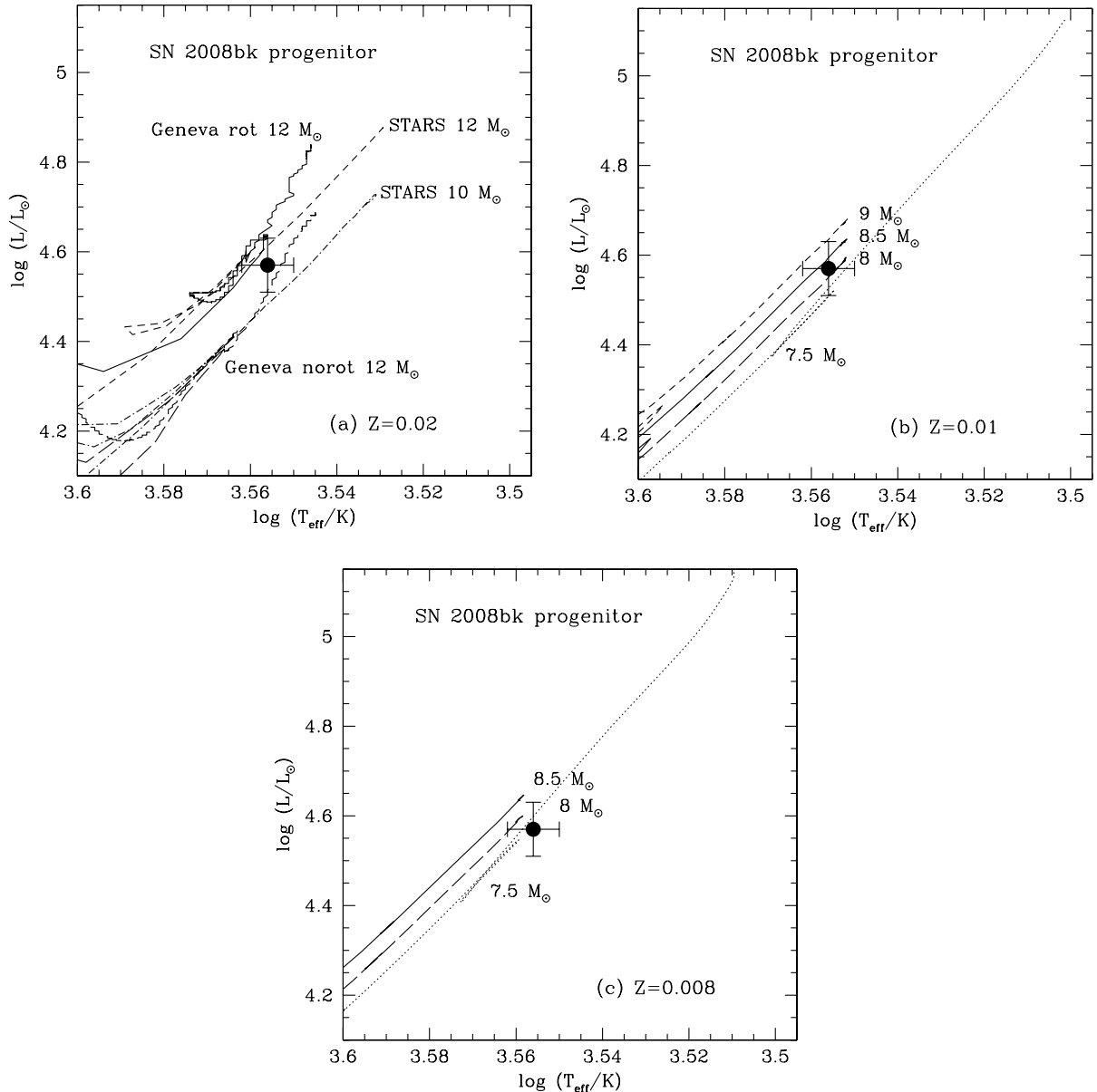


Figure 9. HRD showing the locus of the SN 2008bk progenitor. For comparison, we indicate model stellar evolutionary tracks, in panel (a) at metallicity $Z = 0.02$, in panel (b) at metallicity $Z = 0.01$, and in panel (c) at metallicity $Z = 0.008$. In panel (a), the 12 M_{\odot} models are from Hirschi et al. (2004, “Geneva” models), with rotation (“rot,” $v_{\text{ini}} = 300 \text{ km s}^{-1}$; solid line) and without rotation (“norot”; long-dashed line), and from Eldridge & Tout (2004, “STARS” models), at initial masses 10 M_{\odot} (dot-dashed line) and 12 M_{\odot} (short-dashed line). In panel (b), we show just the STARS models at initial masses 7.5, 8, 8.5, and 9 M_{\odot} (dotted, long-dashed, solid, and short-dashed lines, respectively). In panel (c), we again show just the STARS models at initial masses 7.5, 8, and 8.5 M_{\odot} (dotted, long-dashed, and solid lines, respectively).

in the SN environment is quite this low (Section 4.3). The 8 and 8.5 M_{\odot} tracks terminate with $T_{\text{eff}} = 3615$ and 3622 K, $\log(L_{\text{bol}}/L_{\odot}) = 4.60$ and 4.63, and $R_{\star} = 508$ and 527 R_{\odot} (respectively), which again agree, to within the uncertainties, with the star’s locus in the HRD (the exception being the 7.5 M_{\odot} track, which terminates at a stage too cool and too luminous than what is observed, and again, we can discount it). Much better agreement exists between the star’s properties and the subsolar metallicity tracks, which, all told, imply that the star’s initial mass was $\sim 8\text{--}8.5 M_{\odot}$. These stellar evolutionary models all have lost $\sim 0.3 M_{\odot}$ of mass prior to reaching their termini.

4.5. Comparison with Mattila et al. (2008)

We can make a direct comparison of our results for the SN 2008bk progenitor with those of Mattila et al. (2008). One

can see from Figure 10 that all of our magnitude measurements for the star are $\gtrsim 1\sigma$ brighter than those measured by Mattila et al. (2008), particularly their measurement at I and their upper limit at V (which is substantially fainter than our actual detection in this band). We cannot provide an explanation for this difference. However, we feel confident in the veracity and self-consistency of our photometry, based on comparison with pre-existing photometry of stars in the SN field (Section 2.1), and on the relatively low dispersions in the transformation of $g'r'i'$ photometry to VRI from the Gemini images and of the near-IR instrumental photometry to 2MASS magnitudes from the VLT images (Section 3). Additionally, the Elias et al. (1985) RSG intrinsic colors, specifically $(V - K)_0$, are systematically bluer, for a given T_{eff} and spectral type, than those found by Levesque et al. (2006). The net effect, as seen in Figure 10, is that higher

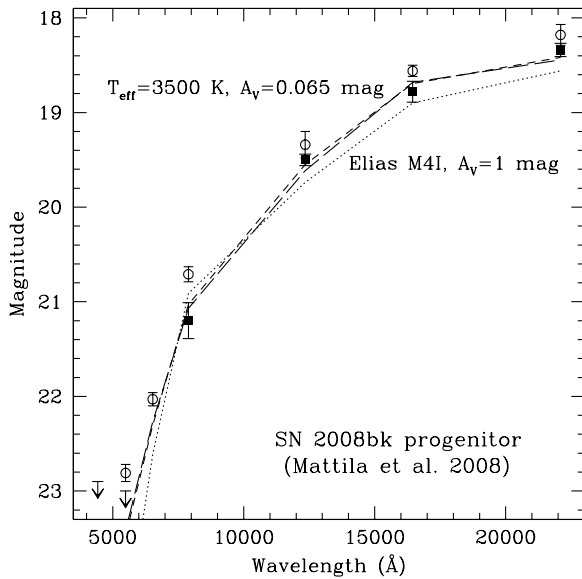


Figure 10. Observed SED of the SN 2008bk progenitor star, as measured by Mattila et al. (2008; filled squares and upper limits). We show the SED we have measured, from Figure 8 (open circles), for comparison. We also display the template SED for an M4I supergiant in the LMC (Elias et al. 1985; dotted line), extinguished by $A_V = 1$ mag (Mattila et al. 2008). Additionally, we illustrate a synthetic SED derived from MARCS model RSG stellar atmospheres (Gustafsson et al. 2008) with $T_{\text{eff}} = 3500$ K at subsolar metallicity ($[M/H] = -0.25$), and with microturbulence velocities of 2 and 5 km s^{-1} (dashed lines), extinguished by our assumed value toward the SN (Section 4.1).

extinction and reddening are required to allow for a comparison (and not a particularly good one) of the model SED for an M4I supergiant from Elias et al. (1985) with the photometry from Mattila et al. (2008). Simply for the sake of argument, we also show in the figure the SED for an RSG from the MARCS stellar atmosphere models with $T_{\text{eff}} = 3500$ K (which Mattila et al. assume to be the equivalent of an M4I star at LMC metallicity), adopting our extinction to the SN. This model actually provides a better comparison with the Mattila et al. (2008) photometry than do the Elias et al. (1985) intrinsic colors, and this not only would imply that the effective temperature is cooler than what we have found but does so in agreement with a far lower value for the extinction than what Mattila et al. (2008) had assumed. The implied cooler temperature is driven primarily by the significantly fainter *I*-band magnitude and upper limit to the *V* brightness found by Mattila et al. (2008).

The fainter *K*-band measurement by Mattila et al. (2008), combined with the implied cooler effective temperature, which corresponds to a larger (positive) BC_K (Levesque et al. 2005, 2006), as well as the lower value for extinction, all lead to a much lower luminosity for the SN progenitor than what we have found to be the case. A comparison of the luminosity and effective temperature with massive-star evolutionary models in an HRD shown in Figure 11 implies that the SN progenitor would have an initial mass well below the threshold mass necessary for core collapse. It is only by virtue of their assumption that $A_V \approx 1.0$ mag, which, based on their photometry, results in the star being more luminous than what we find here, that Mattila et al. arrive at its initial mass being $M_{\text{ini}} \approx 8.5 M_{\odot}$. As we presented in Section 4.1, we have found no evidence for such a large extinction to the SN.

Estimating the reddening to the progenitor through comparison with assumed intrinsic properties for RSGs is almost certainly fraught with uncertainties. Mattila et al. (2008) also

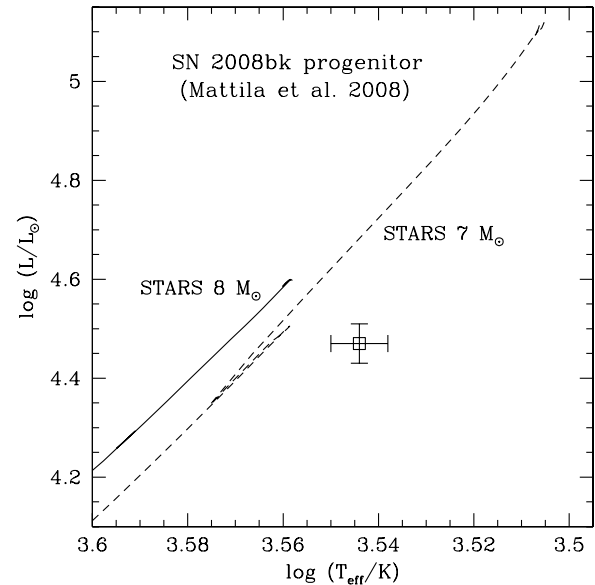


Figure 11. HRD showing the locus of the SN 2008bk progenitor, based on the *K*-band measurement by Mattila et al. (2008), and assuming the overall SED can be modeled by a MARCS model RSG stellar atmosphere (Gustafsson et al. 2008) with $T_{\text{eff}} = 3500$ K at subsolar metallicity ($[M/H] = -0.25$), and further assuming our value of extinction toward the SN (see Figure 10). For comparison, we also show the STARS massive-star evolutionary tracks (Eldridge & Tout 2004), assuming a subsolar metallicity $Z = 0.008$ as Mattila et al. (2008) have, at initial masses 7 and $8 M_{\odot}$ (dashed line and solid line, respectively).

attempted to estimate the extinction based on the Balmer decrement for an H II region (W13; McCall et al. 1985), which is 1/5 from the SN 2008bk site. In general, it is far more accurate to estimate the reddening from the SN light curves and colors, particularly during the plateau phase, where the colors of SNe II-P are remarkably similar (e.g., Bersten & Hamuy 2009). Although our light curves for SN 2008bk are very limited in coverage, we therefore believe that the comparison with the more extensive SN 1999br curves provides a reliable estimate of the extinction to SN 2008bk.

We note that Mattila et al. (2008) assumed the distance modulus from Karachentsev et al. (2003); however, this contributes relatively little to the overall difference between our two studies. Furthermore, our assessments of the metallicity in the SN 2008bk environment differ as well. Mattila et al. (2008) estimated the metallicity, assuming the Pilyugin et al. (2004) metallicity–radial-distance relation for NGC 7793, and concluded that the O abundance was $12 + \log(O/H) = 8.2 \pm 0.1$. Bibby & Crowther (2010) also have determined the metallicity gradient in NGC 7793. If we assume the de-projected radial distance, r , of SN 2008bk given by Mattila et al. (2008; 3.47) and the radial distance at $B = 25$ mag arcsec $^{-2}$, $R_{25} = 4.65$ (Bibby & Crowther 2010, and references therein), then for $r/R_{25} = 0.75$, the abundance is a slightly higher $12 + \log(O/H) = 8.34 \pm 0.05$. We have shown in Section 4.3 from direct estimation of the O abundance in neighboring H II regions that $12 + \log(O/H) \approx 8.4$ – 8.5 .

5. DISCUSSION AND CONCLUSIONS

We conclude that SN 2008bk in NGC 7793 is most likely a low-luminosity SN II-P, similar in characteristics to SN 1999br. We have also confirmed the identification of an RSG as the SN progenitor. This star is readily detected in pre-SN, high-quality

optical images from the Gemini-South Observatory. Although SN 1987A is closer, its association with the star Sk $-69^{\circ}202$ certain, its multi-band brightness and color known (Isserstedt 1975), and, more importantly, its spectral type unambiguously defined (Rousseau et al. 1978), SN 2008bk ranks as the “second best-characterized” SN progenitor identification to date of any SN type. For this reason, its observed properties are well constrained.

We have assumed, based on the photometric comparison with SN 1999br, that the extinction toward SN 2008bk is quite low, $A_V = 0.065$ mag, entirely consistent with Galactic foreground reddening. We have also estimated the metallicity in the SN environment from neighboring H II regions and find that it is consistent with subsolar metallicity ($Z \approx 0.6 Z_{\odot}$). Furthermore, based on comparison of the observed SED with recent models for RSG stellar atmospheres, we are able to assign an effective temperature of $T_{\text{eff}} = 3600 \pm 50$ K, and an absolute bolometric luminosity (relative to the Sun) of $\log(L_{\text{bol}}/L_{\odot}) = 4.57 \pm 0.06$, both quantities with rather small uncertainties. We note the very good agreement in the bolometric magnitudes derived independently from both the observed V and K . Through comparison with recent theoretical massive-star evolutionary models for subsolar metallicity, we conclude that the progenitor of SN 2008bk had an initial mass in the range of $8\text{--}8.5 M_{\odot}$. We note that this inferred mass range is consistent with the upper limit derived for the initial mass of the progenitor of SN 1999br ($<15 M_{\odot}$; Smartt et al. 2009), and is also within the initial mass range for RSG progenitors of SNe II-P, $M_{\text{ini}} = 8.5_{-1.5}^{+1}$ to $16.5 \pm 1.5 M_{\odot}$ (Smartt et al. 2009).

Further constraints on the initial mass of the SN 2008bk progenitor can be obtained through comparison with recent theoretical, radiative-transfer/hydrodynamical simulations of SNe II-P. We can compare our estimate of the star’s radius near explosion, $R_{\star} = 496 \pm 34 R_{\odot}$, to those input to the pre-SN models generated *at solar metallicity* by Dessart et al. (2010b): their nonrotating $11 M_{\odot}$ model has $R_{\star} = 587 R_{\odot}$, while their rotating $10 M_{\odot}$ model has $R_{\star} = 552 R_{\odot}$. This implies that the SN 2008bk progenitor had to be $\lesssim 10 M_{\odot}$, consistent with what we infer from comparison with theoretical massive-star evolutionary tracks.

The low tail-phase luminosity for SNe II of the SN 1999br variety has been explained by a low ^{56}Ni mass produced in the explosion of a lower mass star. As Smartt et al. (2009) point out, nuclear statistical equilibrium is therefore reached only in a thin O–Si-rich layer around the core in such stars. Low progenitor masses are consistent with what has been directly found for other low-luminosity SNe II-P, such as SN 1999br, SN 2003gd in M74 (Van Dyk et al. 2003; Smartt et al. 2004; Hendry et al. 2005), and SN 2005cs (Li et al. 2006; Pastorello et al. 2009). The lower initial mass estimate for the progenitor of SN 2008bk presented here is consistent with this trend and is essentially equivalent to the minimum mass for an SN II-P progenitor (see above; Smartt et al. 2009). It is notable that the case of SN 2008bk offers a possible indication that metallicity could also play a role in the low luminosity. Smartt et al. (2009) assume in the cases of SNe 1999br and 2003gd that the metallicity in these environments was subsolar; on the other hand, they adopt essentially solar metallicity in the case of SN 2005cs. It will be interesting to see in future cases whether a two-parameter (mass and metallicity) trend is possibly emerging.

We have already noted that SN 2008bk is ~ 1.0 mag more luminous than SN 1999br ($M_V^0 = -13.8$ mag; Pastorello et al. 2004). This is particularly surprising, given the close

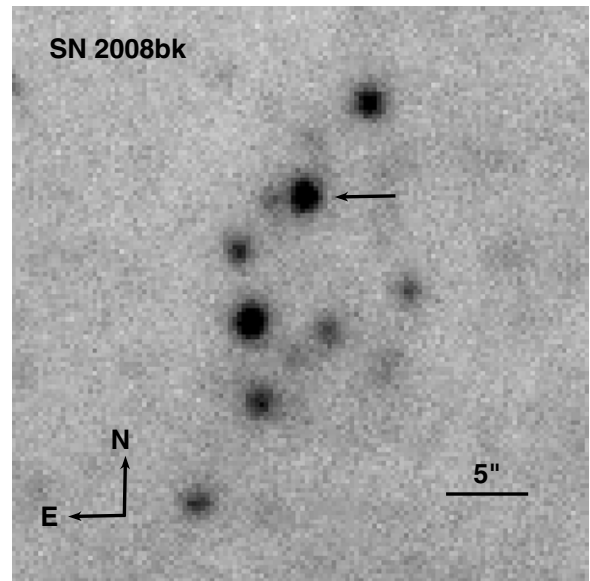


Figure 12. I -band image, obtained on 2009 August 13 at the NOT, showing SN 2008bk (indicated by the arrow) at age ~ 507 days with $I = 18.77$ mag (see Table 2), only ~ 2 mag brighter than the progenitor shown in Figure 6. The scale and orientation here are approximately the same as those in the latter figure. The seeing was $\sim 1''.0$.

overall agreement between the spectra, light-curve shapes, and color evolution for both SNe 1999br and 2008bk; one is tempted to expect their luminosities near maximum brightness to at least be comparable, if not the same (however, see Pastorello et al. 2004 for an assessment of the diversity among low-luminosity SNe II-P). One possible reconciliation of the different luminosities could be to assume a distance to the host galaxy (NGC 4900) of SN 1999br which is different from what has been adopted previously. Pastorello et al. (2004) assumed a “short” distance (17.3 Mpc), which is essentially that derived from the Tully–Fisher relation (Tully 1988); if one adopts the “long” distance (39.5 Mpc) found by Jones et al. (2009) using the expanding photosphere method (EPM), then $M_V^0 = -15.6$ mag, which is now ~ 0.8 mag more luminous than SN 2008bk. Although EPM has its own inherent uncertainties and pitfalls, the implication is that, assuming SNe 2008bk and 1999br are very similar events, the actual distance to the SN 1999br host may be somewhere between the long and short estimates. (Our by-eye adjustment of the SN 1999br light curves in Figure 2 to match those of SN 2008bk would then imply that the distance to NGC 4900 could be ~ 32 Mpc.)

Finally, although it will be ultimately satisfying to validate the identification of the progenitor star by obtaining images of SN 2008bk years hence, when it has faded close to invisibility (e.g., Maund & Smartt 2009),¹⁸ the quality of the pre-SN imaging data and high astrometric precision of the SN and progenitor positions instill in us confidence in the star’s identification. Furthermore, the late-time I image from 2009 August (see Table 2), shown in Figure 12, when compared directly with Figure 6, demonstrates with relatively little doubt that the progenitor is known. As Mattila et al. (2008) point out, in the K_s -band pre-SN image, once the PSF of the RSG was subtracted, a faint source $\sim 0''.5$ south of the SN position remains (we also see this same source when the PSF of the SN is subtracted from the

¹⁸ But note that Dessart et al. (2010a) conjecture that at least some low-luminosity SNe II-P could be SN “impostors,” and therefore the star could survive what might be an outburst, rather than a core-collapse explosion.

late-time *I*-band images). Based on the arguments above, we consider it highly unlikely that this much fainter object is the SN progenitor.

This work is based in part on observations obtained at the Gemini Observatory, which is operated by the Association of Universities for Research in Astronomy, Inc., under a cooperative agreement with the NSF on behalf of the Gemini partnership: the National Science Foundation (United States), the Science and Technology Facilities Council (United Kingdom), the National Research Council (Canada), CONICYT (Chile), the Australian Research Council (Australia), Ministerio da Ciencia e Tecnologia (Brazil), and Ministerio de Ciencia, Tecnologia e Innovacion Productiva (Argentina). It is also based in part on data collected with the 2.2 m telescope of the Calar Alto Observatory (Sierra de Los Filabres, Spain); on observations made with the Nordic Optical Telescope, operated on the island of La Palma jointly by Denmark, Finland, Iceland, Norway, and Sweden, in the Spanish Observatorio del Roque de los Muchachos of the Instituto de Astrofísica de Canarias; and on archival data obtained with the *Spitzer Space Telescope*, which is operated by the Jet Propulsion Laboratory, California Institute of Technology under a contract with NASA.

We thank A. Pastorello for the reductions of the CTIO spectra. We are also grateful to S. Larsen for the photometric calibration of his Danish telescope images of NGC 7793. The SN 1999br spectrum was obtained from the Padova-Asiago Supernova Archive. This research also utilized the NASA/IPAC Extragalactic Database (NED), which is operated by the Jet Propulsion Laboratory, California Institute of Technology, under contract with NASA. A.V.F. and W.L. are grateful for the support of NSF grant AST-0908886 and the TABASGO Foundation. M.H. acknowledges support by Proyecto Regular Fondecyt 1060808. M.H. and G.P. acknowledge partial support from Centro de Astrofísica FONDAP 15010003, Center of Excellence in Astrophysics and Associated Technologies PFB 06, and by Programa Iniciativa Científica Milenio de MIDEPLAN (grant P06-045-F).

REFERENCES

- Aldering, G., Humphreys, R. M., & Richmond, M. W. 1994, *AJ*, **107**, 662
- Asplund, M., Grevesse, N., Sauval, A. J., Allende Prieto, C., & Kiselman, D. 2004, *A&A*, **417**, 751
- Bersten, M. C., & Hamuy, M. 2009, *ApJ*, **701**, 200
- Bertola, F. 1964, *Ann. Astrophys.*, **27**, 319
- Bessell, M. S., & Brett, J. M. 1988, *PASP*, **100**, 1134
- Bibby, J. L., & Crowther, P. A. 2010, *MNRAS*, **405**, 2737
- Cardelli, J. A., Clayton, G. C., & Mathis, J. S. 1989, *ApJ*, **345**, 245
- Carpenter, J. M. 2001, *AJ*, **121**, 2851
- Cohen, J. G., Darling, J., & Porter, A. 1995, *AJ*, **110**, 308
- Crampton, D., Fletcher, J. M., Jean, I., et al. 2000, *Proc. SPIE*, **4008**, 114
- Denicoló, G., Terlevich, R., & Terlevich, E. 2002, *MNRAS*, **330**, 69
- Dessart, L., Livne, E., & Waldman, R. 2010a, *MNRAS*, **405**, 2113
- Dessart, L., Livne, E., & Waldman, R. 2010b, *MNRAS*, **408**, 827
- Eldridge, J. J., & Tout, C. A. 2004, *MNRAS*, **348**, 201
- Elias, J. H., Frogel, J. A., & Humphreys, R. M. 1985, *ApJS*, **57**, 91
- Elmhamdi, A., Danziger, I. J., Chugai, N., et al. 2003, *MNRAS*, **338**, 939
- Fraser, M., Ergon, M., Eldridge, J. J., et al. 2011, *MNRAS*, **417**, 1417
- Gilmozzi, R., Cassatella, A., Clavel, J., et al. 1987, *Nature*, **328**, 318
- Gustafsson, B., Edvardsson, B., Eriksson, K., et al. 2008, *A&A*, **486**, 951
- Hamuy, M., Pinto, P. A., Maza, J., et al. 2001, *ApJ*, **558**, 615
- Heger, A., Fryer, C. L., Woosley, S. E., Langer, N., & Hartmann, D. H. 2003, *ApJ*, **591**, 288
- Hendry, M. A., Smartt, S. J., Maund, J. R., et al. 2005, *MNRAS*, **359**, 906
- Hirschi, R., Meynet, G., & Maeder, A. 2004, *A&A*, **425**, 649
- Humphreys, R. M., & McElroy, D. B. 1984, *ApJ*, **284**, 565
- Isserstedt, J. 1975, *A&AS*, **19**, 259
- Jacobs, B. A., Rizzi, L., Tully, R. B., et al. 2009, *AJ*, **138**, 332
- Jones, M. I., Hamuy, M., Lira, P., et al. 2009, *ApJ*, **696**, 1176
- Karachentsev, I. D., Grebel, E. K., Sharina, M. E., et al. 2003, *A&A*, **404**, 93
- Kennicutt, R. C., Jr., Armus, L., Bendo, G., et al. 2003, *PASP*, **115**, 928
- Kochanek, C. S., Szczygiel, D. M., & Stanek, K. Z. 2011, *ApJ*, **737**, 76
- Larsen, S. S. 1999, *A&AS*, **139**, 393
- Larsen, S. S., & Richtler, T. 1999, *A&A*, **345**, 59
- Leonard, D. C., Filippenko, A. V., Gates, E. L., et al. 2002, *PASP*, **114**, 35
- Leonard, D. C., Kanbur, S. M., Ngeow, C. C., & Tanvir, N. R. 2003, *ApJ*, **594**, 247
- Levesque, E. M., Massey, P., Olsen, K. A. G., et al. 2005, *ApJ*, **628**, 973
- Levesque, E. M., Massey, P., Olsen, K. A. G., et al. 2006, *ApJ*, **645**, 1102
- Li, W., Bloom, J. S., Podsiadlowski, P., et al. 2011, *Nature*, in press (arXiv:1109.1593)
- Li, W., Van Dyk, S. D., Filippenko, A. V., et al. 2006, *ApJ*, **641**, 1060
- Li, W., Van Dyk, S. D., Filippenko, A. V., et al. 2008, *CBET*, **1319**, 1
- Maoz, D., & Mannucci, F. 2008, *ATel*, **1464**, 1
- Matheson, T., Filippenko, A. V., Barth, A. J., et al. 2000, *AJ*, **120**, 1487
- Mattila, S., Smartt, S. J., Eldridge, J. J., et al. 2008, *ApJ*, **688**, L91
- Maund, J. R., & Smartt, S. J. 2009, *Science*, **324**, 486
- Maund, J. R., Smartt, S. J., & Danziger, I. J. 2005, *MNRAS*, **364**, L33
- McCall, M. L., Rybski, P. M., & Shields, G. A. 1985, *ApJS*, **57**, 1
- Monard, L. A. G. 2008, *CBET*, **1315**, 1
- Morrell, N., & Stritzinger, M. 2008, *CBET*, **1335**, 1
- Mould, J., & Sakai, S. 2008, *ApJ*, **686**, L75
- Nomoto, K., Tominaga, N., Umeda, H., Kobayashi, C., & Maeda, K. 2006, *Nucl. Phys. A*, **777**, 424
- Pastorello, A., Valenti, S., Zampieri, L., et al. 2009, *MNRAS*, **394**, 2266
- Pastorello, A., Zampieri, L., Turatto, M., et al. 2004, *MNRAS*, **347**, 74
- Pettini, M., & Pagel, B. E. J. 2004, *MNRAS*, **348**, L59
- Pierce, M. J., & Tully, R. B. 1992, *ApJ*, **387**, 47
- Pietrzyński, G., Gieren, W., Hamuy, M., et al. 2010, *AJ*, **140**, 1475
- Pignata, G., Maza, J., Hamuy, M., et al. 2008, *CBET*, **1319**, 2
- Pilyugin, L. S., Vílchez, J. M., & Contini, T. 2004, *A&A*, **425**, 849
- Puche, D., & Carignan, C. 1988, *AJ*, **95**, 1025
- Rizzi, L., Tully, R. B., Makarov, D., et al. 2007, *ApJ*, **661**, 815
- Rousseau, J., Martin, N., Prévot, L., et al. 1978, *A&AS*, **31**, 243
- Russell, S. C., & Dopita, M. A. 1990, *ApJS*, **74**, 93
- Ryder, S., Staveley-Smith, L., Dopita, M., et al. 1993, *ApJ*, **416**, 167
- Schlegel, D. J., Finkbeiner, D. P., & Davis, M. 1998, *ApJ*, **500**, 525
- Smartt, S. J., Eldridge, J. J., Crockett, R. M., & Maund, J. R. 2009, *MNRAS*, **395**, 1409
- Smartt, S. J., Maund, J. R., Hendry, M. A., et al. 2004, *Science*, **303**, 499
- Smith, N., Li, W., Silverman, J. M., Ganeshalingam, M., & Filippenko, A. V. 2011, *MNRAS*, **415**, 773
- Sonneborn, G., Altner, B., & Kirshner, R. P. 1987, *ApJ*, **323**, L35
- Stetson, P. B. 1987, *PASP*, **99**, 191
- Storchi-Bergmann, T., Calzetti, D., & Kinney, A. L. 1994, *ApJ*, **429**, 572
- Terlevich, R., Melnick, J., Masegosa, J., Moles, M., & Copetti, M. V. F. 1991, *A&A*, **91**, 285
- The DENIS Consortium 2005, *VizieR Online Data Catalog*, **2263**, 0
- Tonry, J. L., Dressler, A., Blakeslee, J. P., et al. 2001, *ApJ*, **546**, 681
- Tully, R. B. 1988, *Nearby Galaxies Catalog* (Cambridge: Cambridge Univ. Press) (*VizieR Online Data Catalog*, **7145**, 0)
- Turatto, M., Mazzali, P. A., Young, T. R., et al. 1998, *ApJ*, **498**, L129
- Van Dyk, S. D. 2005, in *ASP Conf. Ser.* **332**, The Fate of the Most Massive Stars, ed. R. Humphreys & K. Stanek (San Francisco, CA: ASP), **47**
- Van Dyk, S. D., Garnavich, P. M., Filippenko, A. V., et al. 2002, *PASP*, **114**, 1322
- Van Dyk, S. D., Li, W., & Filippenko, A. V. 2003, *PASP*, **115**, 1289
- Van Dyk, S. D., & Matheson, T. 2011, *ApJ*, submitted
- Welch, D. L., Clayton, G. C., Campbell, A., et al. 2007, *ApJ*, **669**, 525
- Woosley, S. E., & Weaver, T. A. 1986, *ARA&A*, **24**, 205
- Zampieri, L., Pastorello, A., Turatto, M., et al. 2003, *MNRAS*, **338**, 711
- Zwicky, F. 1964, *ApJ*, **139**, 514